

1

2

Journal of Geophysical Research: Solid Earth

3

Supporting Information for

4

**Three-Dimensional S-Wave Velocity Structure of the Kinki Region, Southwestern
5 Japan based on Ambient Seismic Noise Tomography using Data from Dense
6 Seismic Array**

6

7

B. Nthaba^{1,2}, T. Ikeda^{1,3}, H. Nimiya^{1,4}, T. Tsuji^{1,3}, and Y. Iio⁵

8

¹ Department of Earth Resources Engineering, Kyushu University, Fukuoka, Japan,

9

² Earth and Environmental Sciences Department, Botswana International University of Science and
10 Technology, P/Bag 16, Palapye, Botswana,

10

11

³ International Institute for Carbon-Neutral Energy Research, Kyushu University, Fukuoka, Japan,

12

⁴ Geological Survey of Japan, National Institute of Advanced Industrial Science and Technology (AIST),
13 Ibaraki, Japan,

13

14

⁵ Disaster Prevention Research Institute, Kyoto University, Kyoto, Japan.

15

16

17

Contents of this file

18

19

Figures S1 to S7

20

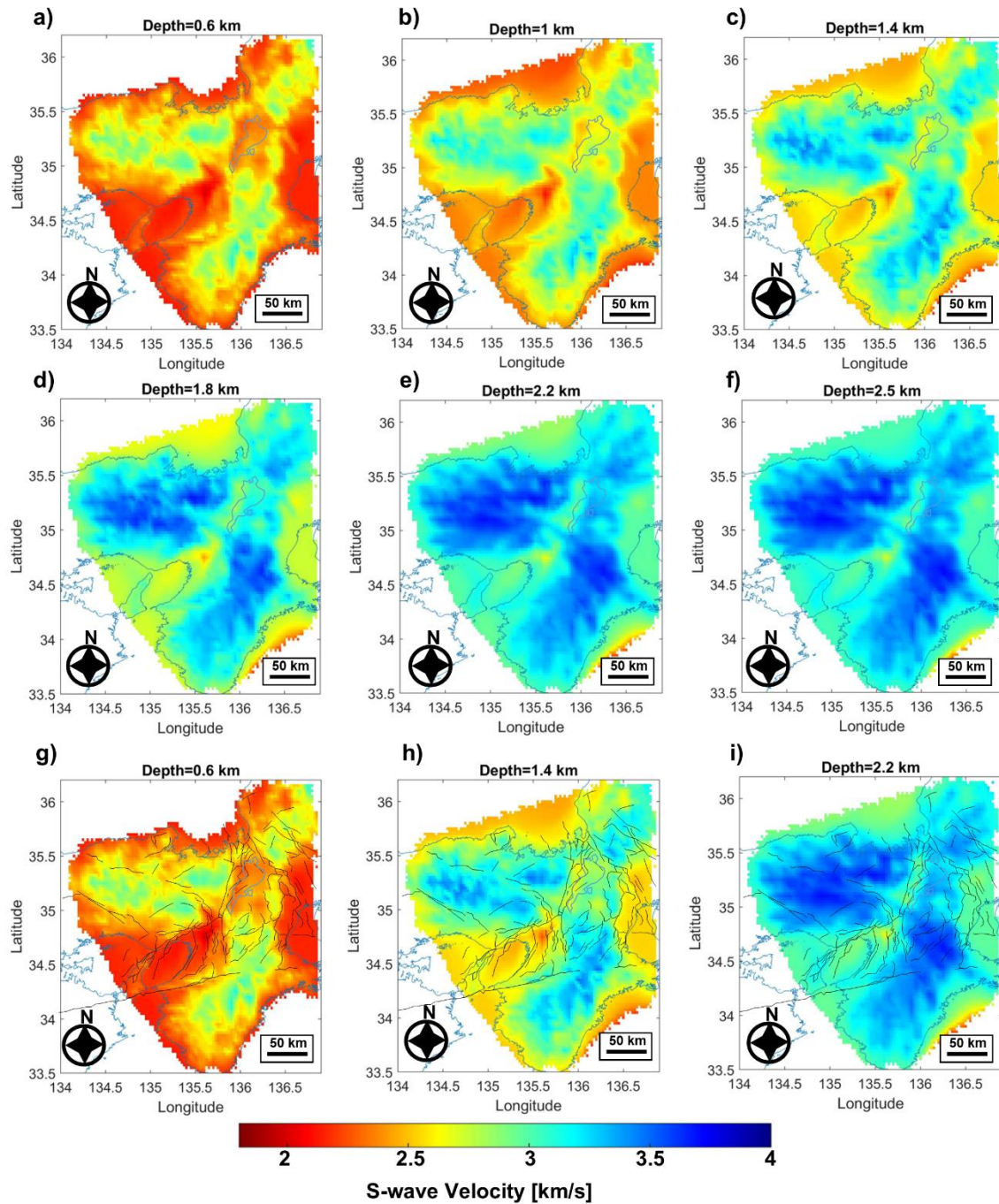
21

Introduction

22

Supplementary figures referred to in the main text are provided in this document.

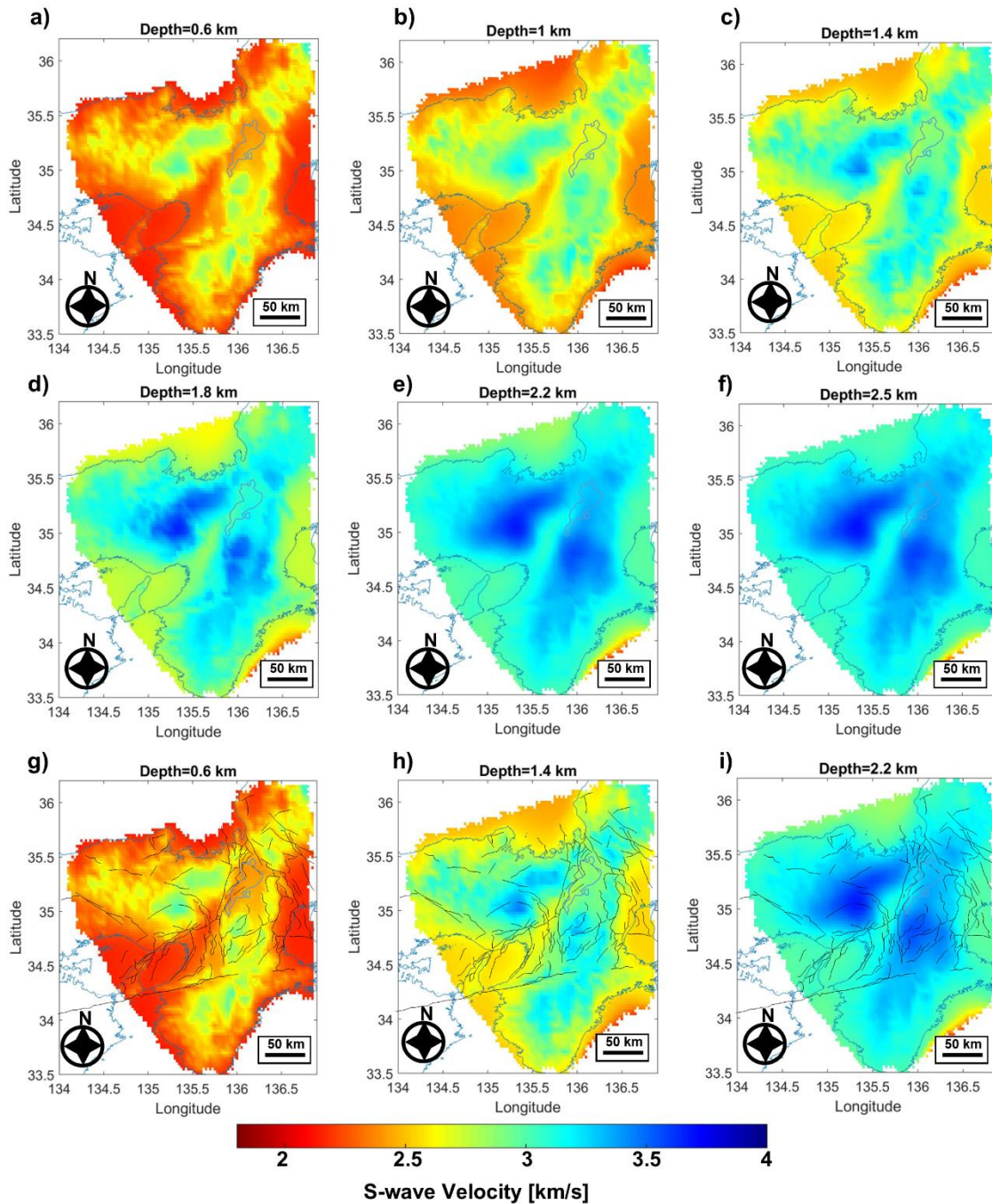
23



24

25 **Figure S1.** Weakly smoothed S-wave velocity models at different depths below sea level,
 26 given above each panel. (a–f) S-wave velocity models without showing the active faults.
 27 (g–i) S-wave velocity models overlaid with active faults (black lines).

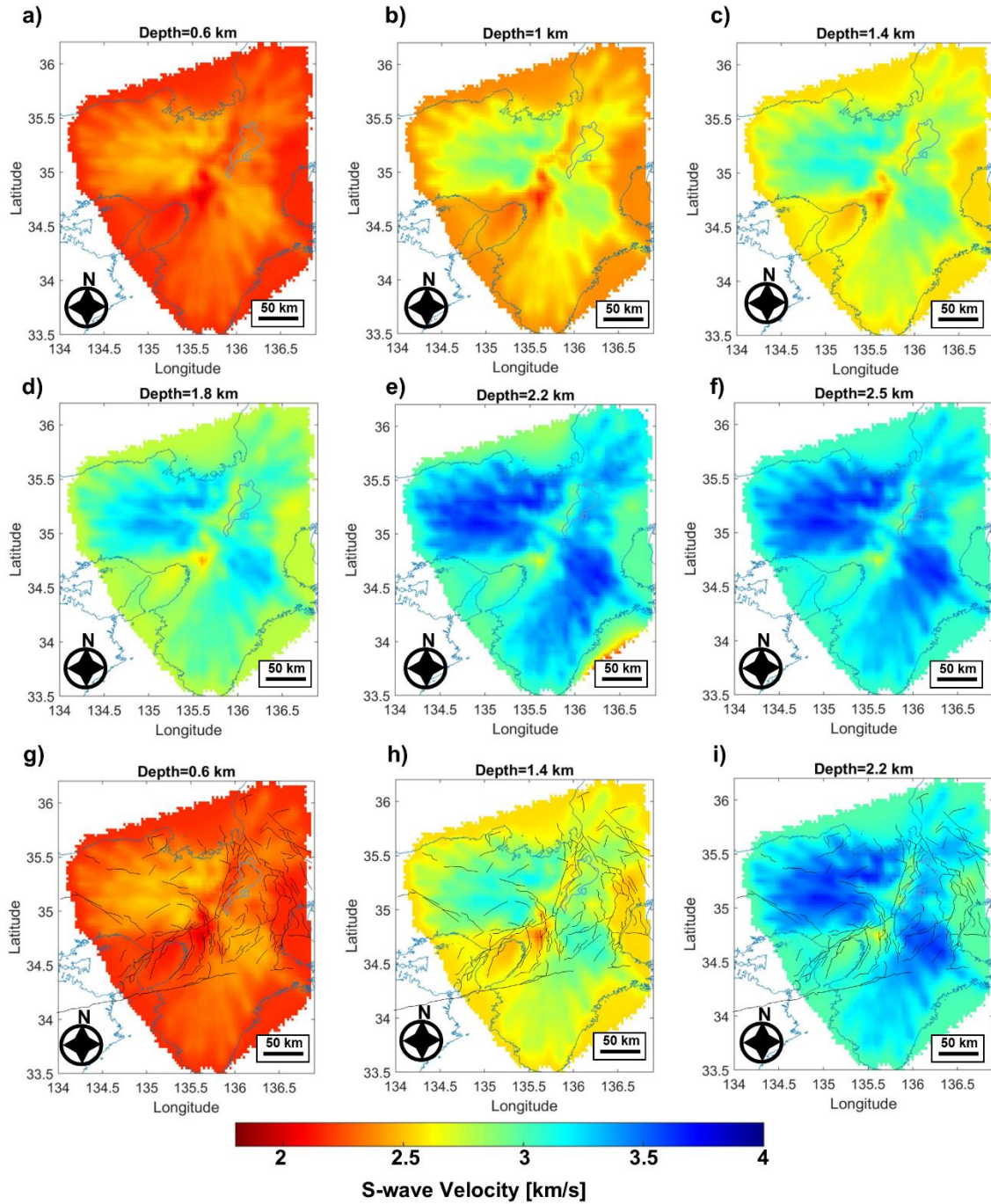
28



29

30 **Figure S2.** Strongly smoothed S-wave velocity models at different depths below sea
 31 level, given above each panel. (a–f) S-wave velocity models without showing the active
 32 faults. (g–i) S-wave velocity models overlaid with active faults (black lines).

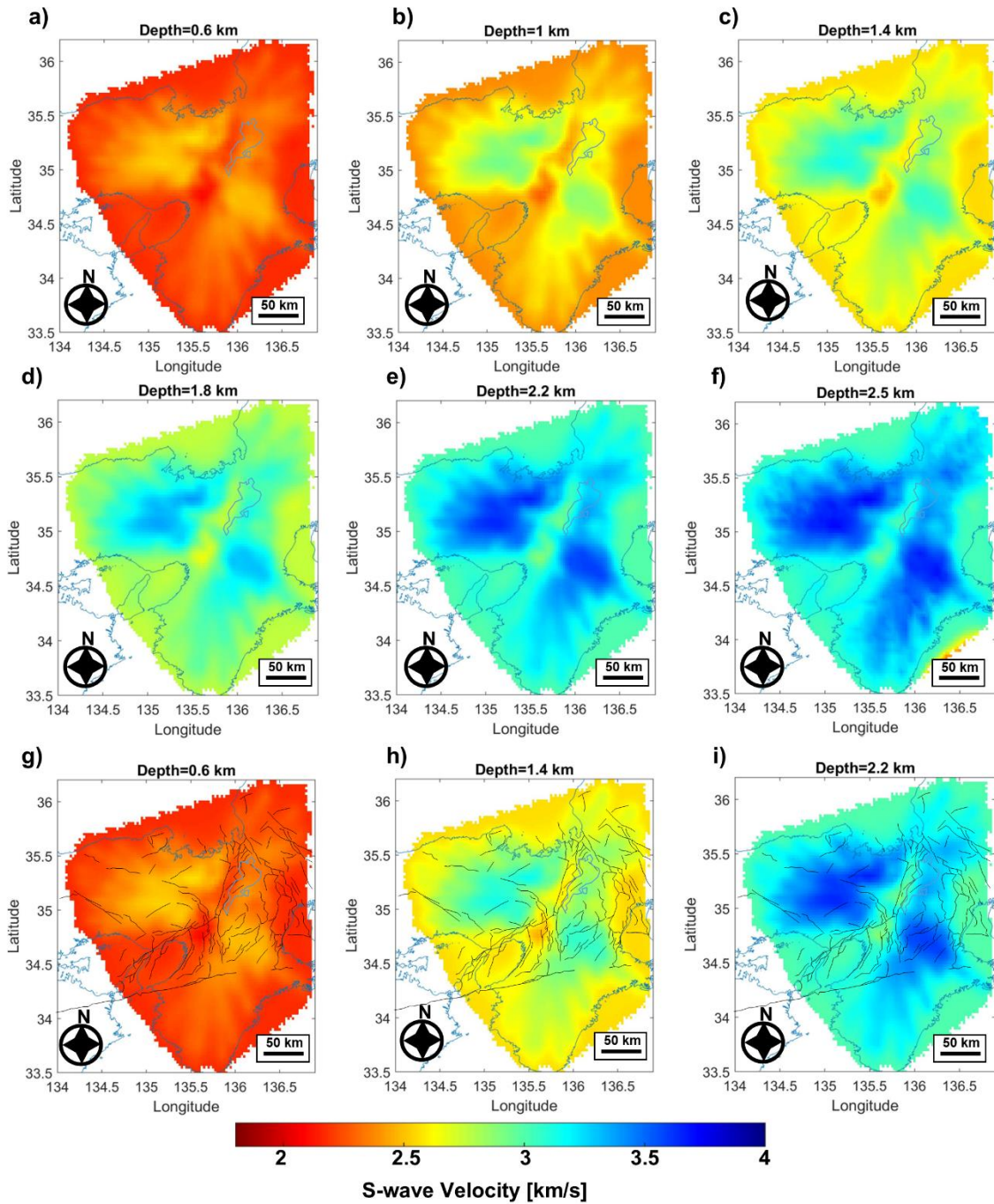
33



34

35 **Figure S3.** Weakly smoothed S-wave velocity models at different depths before
 36 topographic correction. (a–f) S-wave velocity models without showing the active faults.
 37 (g–i) S-wave velocity models overlaid with active faults (black lines).

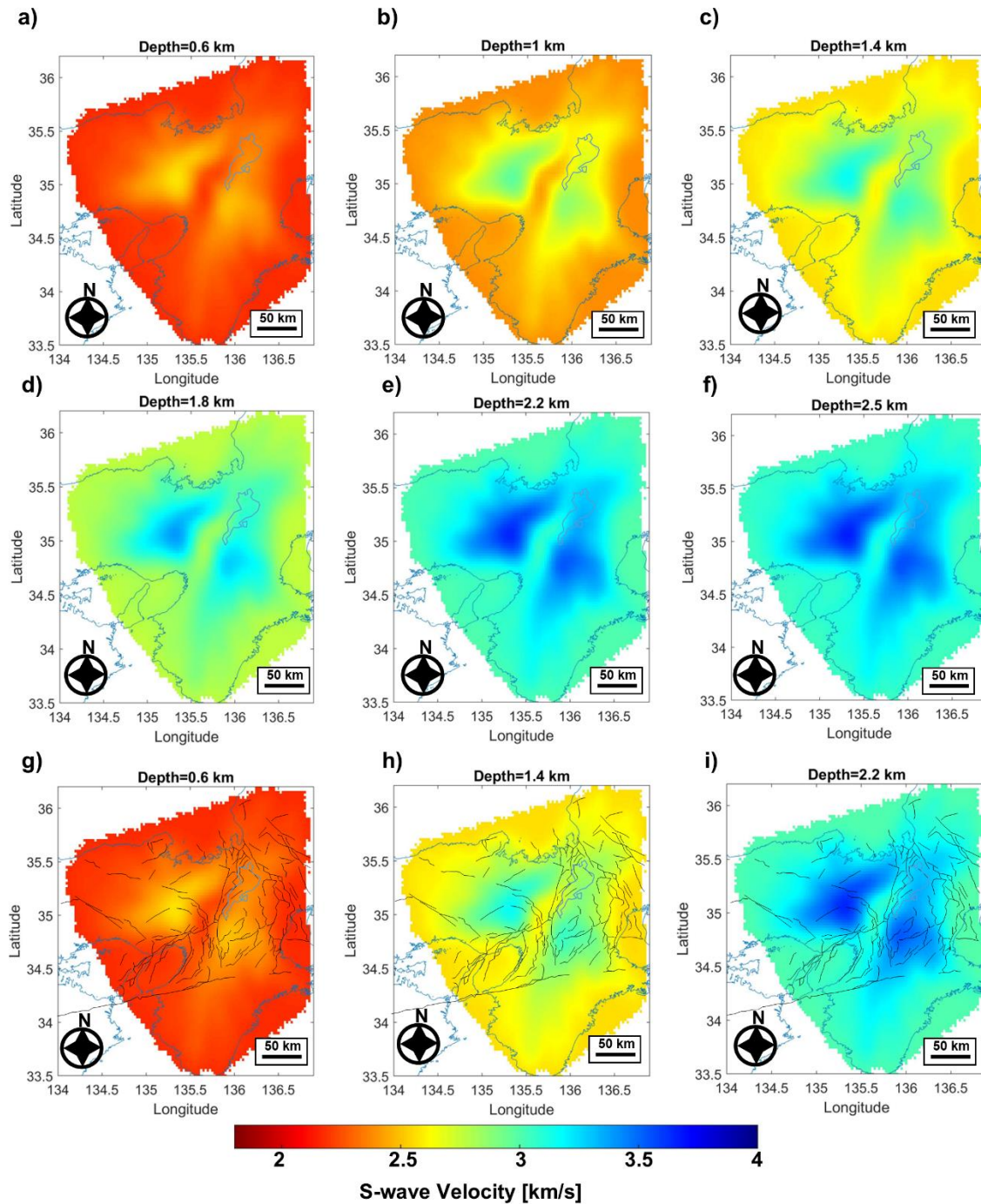
38



39

40 **Figure S4.** Moderately smoothed S-wave velocity models at different depths before
 41 topographic correction. (a–f) S-wave velocity models without showing the active faults.
 42 (g–i) S-wave velocity models overlaid with active faults (black lines).

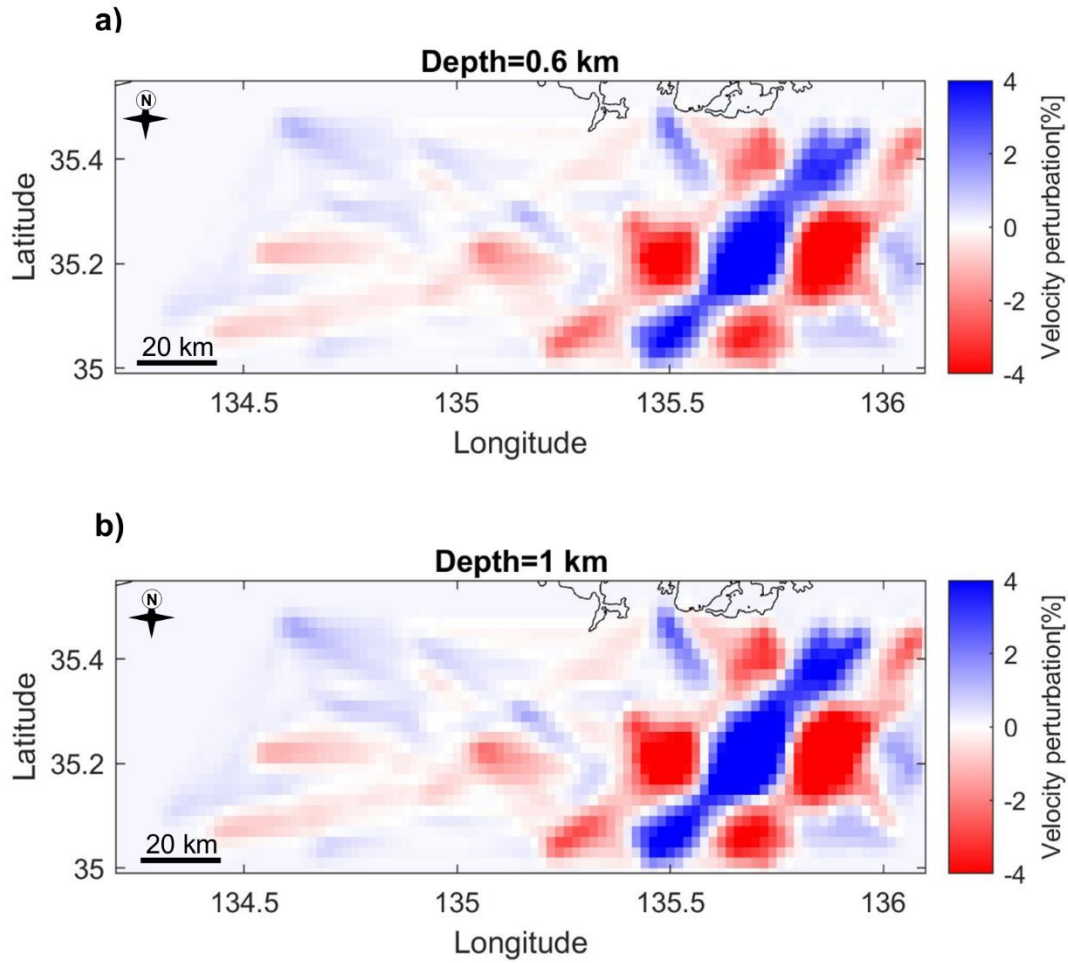
43



44

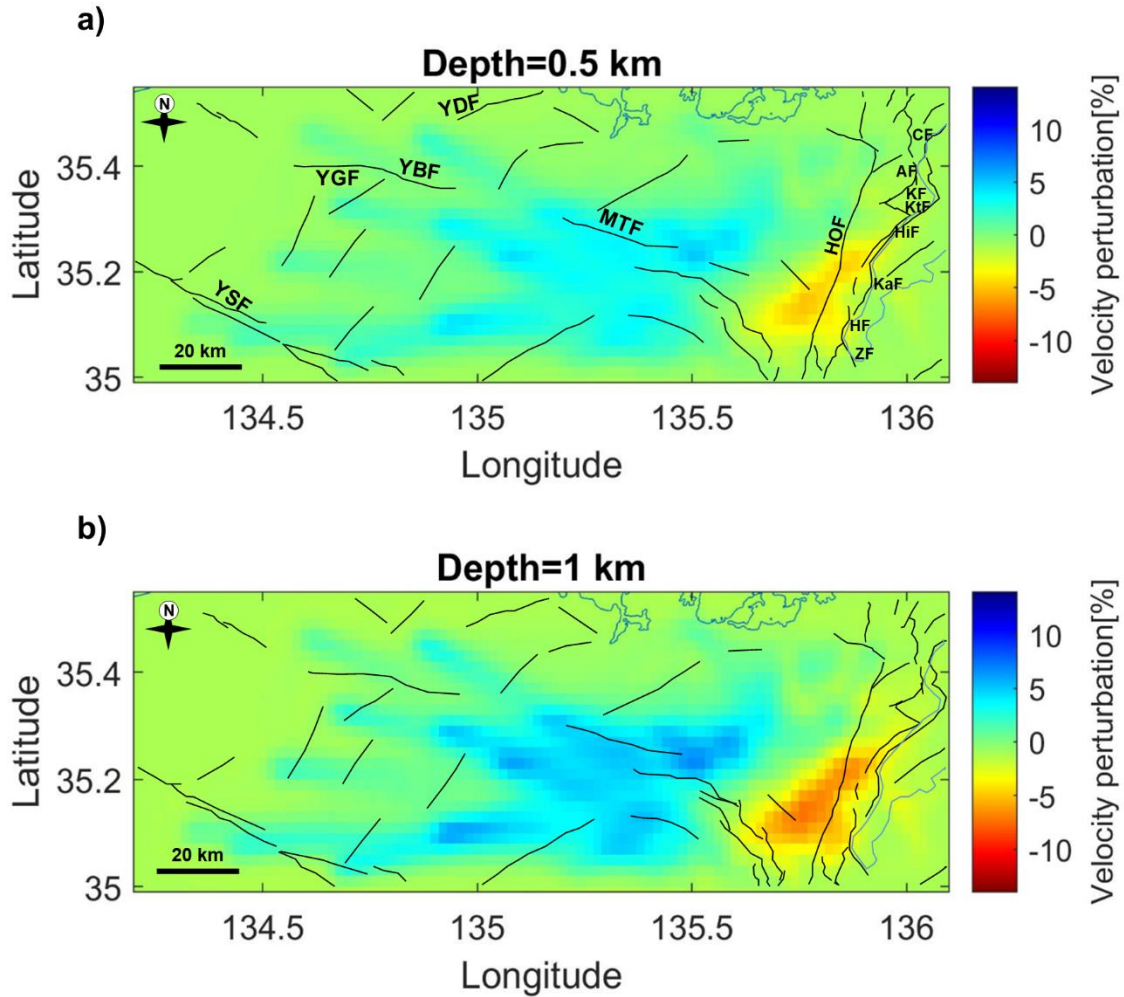
45 **Figure S5.** Strongly smoothed S-wave velocity models at different depths before
 46 topographic correction. (a–f) S-wave velocity models without showing the active faults.
 47 (g–i) S-wave velocity models overlaid with active faults (black lines).

48



49

50 **Figure S6.** Horizontal velocity perturbation slices of the checkerboard resolution test
 51 results for the northern part of the Kinki region at 0.6 km (a) and 1 km (b) depths. The
 52 anomaly size was ~ 11 km (0.1°), and the velocity amplitude was $\sim 10\%$. Depth is shown
 53 above each horizontal slice.



54

55 **Figure S7.** S-wave velocity perturbation of the northern part of the Kinki region before
 56 topographic correction. (a) S-wave velocity perturbation at a depth of 0.5 km below sea
 57 level. Also shown are the locations of the Yamada Fault (YDF), Yamasaki Fault (YSF), Yagi-
 58 Yabu Fault (YGF-YBF), Mitoke Fault (MTF), Hanaore Fault (HOF) and the Biwako-seigan
 59 Fault Zone members (Chinai Fault, CF; Aibano Fault, AF; Kamidera Fault, KF; Katsuno, KtF;
 60 Hira Fault, HiF; Katata, KaF; Hiei Fault, HF; Zeze Fault, ZF). (b) S-wave velocity perturbation
 61 at a depth of 1 km below sea level. Solid black lines represent documented active faults.

62